Abdominal Imaging

Published online: 1 August 2006

Abdom Imaging (2006) 31:632–643
DOI: 10.1007/s00261-006-9022-2

Cross-sectional imaging of nodal metastases in the abdomen and pelvis

D. M. Koh, M. Hughes, J. E. Husband

Academic Department of Radiology, Royal Marsden Hospital, Downs Road, Sutton SM2 5PT, UK

Abstract

Accurate nodal staging is important for the management of patients with abdominal and pelvic malignancies. Local and nodal staging using cross-sectional imaging can influence treatment planning. The measurement of nodal size is still the most widely used criteria for discriminating between benign and malignant nodes. However, knowledge of the pathways of nodal spread, the treatment history, and careful analysis of nodal characteristics can improve nodal assessment. An appreciation of normal structures that may simulate nodal disease is also important. The potential for further improving nodal staging accuracy by positron emission tomography and magnetic resonance lymphography is discussed.

Key words: Abdomen—Nodes—Pelvis—Staging

Cross-sectional computed tomoraphy (CT) and magnetic resonance imaging (MRI) are the most widely used imaging techniques for the assessment of nodal disease in the patient with cancer. CT and MR examination enables direct visualization of lymph nodes, allowing evaluation of these nodes in relation to the primary tumor.

Nodal enlargement occurs as a nonspecific response to a variety of disease. Not surprisingly, there is a substantial overlap in the size and appearances of lymph nodes involved by benign and malignant diseases. Furthermore, metastases not infrequently spread to nodes that are not enlarged by conventional criteria [1]. Thus, the keys to successful interpretation of cross-sectional imaging for nodal diseases rely on a good understanding of the disease entities, their pattern of nodal involvement, and their characteristic features on imaging.

Correspondence to: D. M. Koh; *email:* dowmukoh@icr.ac.uk

Normal lymph nodes in the abdomen and pelvis

Lymph nodes within the retroperitoneum are named and grouped according to their relation to the inferior vena cava and the abdominal aorta: paracaval, precaval, retrocaval, aortocaval, preaortic, and paraortic. These nodes lie along the major lumbar lymphatic trunks, which receive lymphatic drainage from the lower limbs and the pelvis. In the pelvis, lymph nodes along the pelvis sidewall can be divided into the following groups: common iliac, external iliac (including obturator), hypogastric (along the internal iliac vessels), and presacral. Lymphatics associated with these nodal groups drain upward into the retroperitoneum. Lymphatics associated with the pelvic viscera can also drain externally into the inguinal nodes.

There are also lymph nodes associated with abdominal viscera. These are found along the distribution of the coeliac axis, superior mesenteric artery, and inferior mesenteric artery. Nodes related to the celiac axis include those along the great and lesser curvatures of the stomach, those at the portal hepatis, and pancreaticoduodenal nodes. Mesenteric nodes are found between the layers of the small bowel mesentery at the root of the superior mesenteric artery. Using multidetector CT, normal nodes in these locations may be identified, especially when the images are viewed on a workstation. For example, mesenteric lymph nodes < 5 mm in diameter are frequently found in asymptomatic normal individuals (Fig. 1) using multidetector CT [2]. The majority of these are found at the mesenteric root, but some may be seen in the mesenteric periphery or within the right iliac fossa [2]. Lymph nodes can also be identified in the distribution of the inferior mesenteric artery, within the sigmoid mesentery, and along the superior rectal vessels. Lymphatics from the abdominal viscera ultimately drain into the retroperitoneum and via the cisterna chyli into the thorax.

On CT imaging, normal nodes are ovoid in shape and are of soft tissue density. These can be clearly visualized

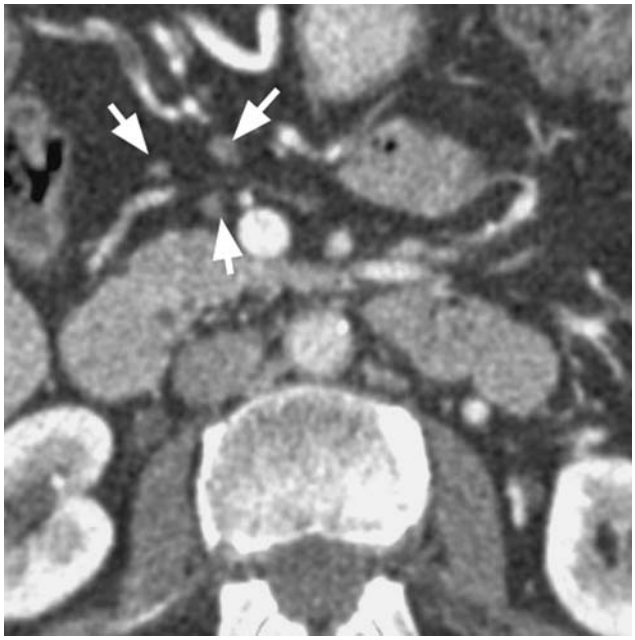

Fig. 1. The use of multidetector CT allows normal mesenteric nodes (*arrows*), normally measuring about 5 mm in diameter, to be confidently detected.

by using thin-section or multidetector CT and viewing the images on a workstation. A slice section thickness of 2–3 mm is ideal for nodal assessment and allows multiplanar reformats. On MRI, nodes are typically isointense to muscle on T1-weighted MRI and are isointense or mildly hyperintense on T2-weighted MRI (Fig. 2). On short-tau inversion recovery (STIR) sequence, nodes appear very high in signal intensity, which can aid in their identification. However, the choice of the MR sequence for nodal identification and assessment varies with the anatomical region and individual preference. A combination of high–spatial resolution T1- and T2-weighted sequences is usually employed. High–spatial resolution, turbo-spin echo T2-weighted [3] and three-dimensional (3D) T1-weighted MP-RAGE [4] sequences have been found to be particularly useful in some instances.

Until recently, the only widely accepted method of discriminating between normal and pathological nodes is based on nodal size. The maximum short-axis nodal diameter is usually ascertained. However, the size of normal nodes varies within anatomical location in the body. In the abdomen, the upper limit of the maximum short-axis diameter of normal nodes varies between 6 and 10 mm, increasing in size caudally [5, 6]. For example, it is generally accepted that the upper limit in the maximum short-axis diameter of a normal retrocrural node is 6 mm and that of a retroperitoneal abdominal node is 10 mm [7]. In the pelvis, normal nodes are usually < 10 mm in diameter [7, 8]. The mean maximum short-axis diameter of normal inguinal nodes varies between 4 and 6 mm but can measure up to 15 mm [5, 9]. The upper limit of the mean maximum short-axis diameters of nodes according to anatomical regions in the abdomen and pelvis are summarized in Table 1 [5–8, 10–12]. However, there may be variations in the application of these criteria to determine whether nodes are normal or abnormal according to practice and tumor types.

Cross-sectional nodal imaging in the patient with cancer

The presence of nodal metastases is an adverse prognostic factor in patients with abdominal and pelvic malignancy. The presence of nodal disease can alter management decisions, which include the choice of surgery, chemotherapy, and radiotherapy. Nodal disease is frequently an independent poor prognostic factor in patient survival. This has been shown to be true in gastric, renal, colorectal, prostate, bladder, cervical, endometrial, and ovarian cancers. The recurrence rate of cancer is also increased with nodal spread.

Nevertheless, the overall accuracy of CT and MRI in nodal staging is limited. This is largely due to the fact that metastases frequently involve nodes that are not enlarged according to conventional criteria. However, improvement in results can be achieved by careful consideration of factors relevant to the primary tumor.

Stage, grade, histology, and biology of the primary cancer

In most abdominal and pelvic cancers, the incidence of nodal disease increases with the stage of the primary tumor. For example, in patients with prostate cancer, patients with organ-confined disease (TNM stage T1/T2) have $< 5\%$ incidence of nodal metastasis, compared to 30% for patients with extracapsular spread of disease (stage T3) [13–15]. The relationship between the stage of the tumor and the likelihood of nodal metastasis in prostate, colorectal, bladder, and ovarian cancers is summarized in Table 2.

The grade and other histological characteristics of tumors also have a bearing on the likelihood of nodal metastases. In cervical cancer, the presence of parametrial invasion and lymphovascular invasion and the depth of tumor invasion are linked to the presence of nodal disease [16]. In early gastric cancer, the presence of submucosal and vascular invasion predicts the likelihood of nodal disease [17]. Lymphovascular invasion also increases the risk of nodal disease in patients with colorectal cancer [18] and testicular tumors [19, 20].

Other biological indexes can help to alert radiologists to the likelihood of nodal metastases. In patients with prostate cancer, patients expressing high levels of prostate specific antigen in the serum (> 20 ng/ml) and have a high Gleason score (> 7) on prostate biopsy have a

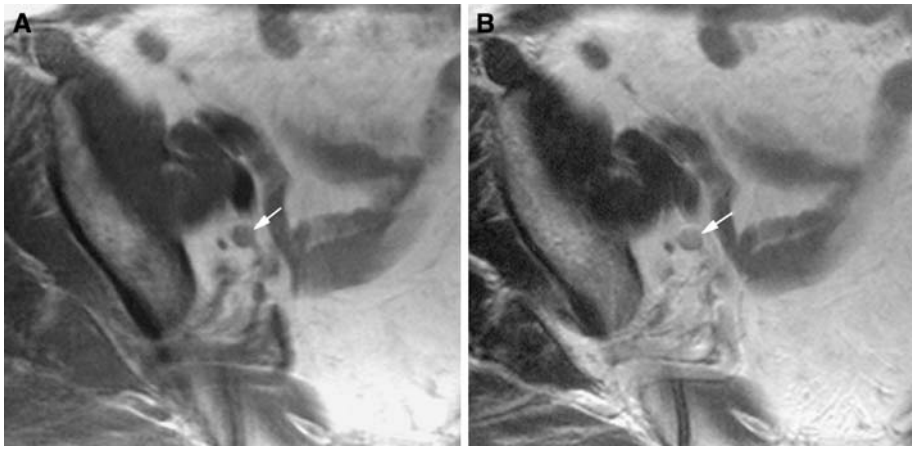

Fig. 2. (**A**) T1-weighted and (**B**) T2-weighted MRI showing an 8-mm hypogastric node along the right pelvic sidewall (*arrows*) in a 60-year-old man with prostate cancer. The node shows near isointensity to muscle on T1-weighted imaging and appears mildly hyperintense on T2-weighted imaging. MRI can identify a greater number of normal nodes compared to CT imaging.

Table 1. The upper limit of normal of nodal size according to anatomical regions in the abdomen and pelvis

Site	Nodal size (mm)[a]
Retrocrual	6
Paracardiac	12
Gastrohepatic	8
Porta hepatis	7
Portacaval	10 (13[b])
Upper paraortic	9
Lower paraortic	11
Mesenteric	5
Pelvic	10
Inguinal	15

[a]Based on Refs. 5–8 and 10–12
[b]Refer to Ref. 12

Table 2. Examples of the increasing incidence of nodal disease with increasing local tumor stage [14, 61–63]

	Incidence of nodal disease			
	T1	T2	T3	T4
Prostate	< 5%	< 5%	15% (Early) 30% (T3)	> 40%
Bladder	< 5%	10%–15% (T2a) 15%–20% (T2b)	30%–50%	40%–45%
Colorectal	3%–10%	10%–30%	> 50%	> 50%
Ovarian	5%–20%	5%–20%	30%–40%	> 50%

higher risk of extracapsular prostatic disease and nodal disease. In patients with prostate cancer, reference to the Partin normograms can be helpful to the radiologist [21]. These nomograms are based on the preoperative serum prostate specific antigen, clinical TNM stage, and biopsy Gleeson score, which are predictive of the histopathological staging at radical prostatectomy and the likelihood of nodal disease. Hence, a high risk of nodal disease according to the Partin nomograms should alert the radiologist to careful nodal survey.

Patterns of tumor spread

A clear understanding of the pathway of tumor spread allows close scrutiny of the most likely sites of nodal

Fig. 3. CT imaging showing the typical site of nodal involvement in a man with a locally advanced prostatic carcinoma. Note the enlarged obturator (*asterisk*) and external iliac nodes (*arrow*).

involvement. Prostate carcinoma typically spreads via lymphatics in the neurovascular bundles to the obturator, presacral, hypogastric, and external iliac lymph nodes. Further spread is to the common iliac and paraortic nodes. The obturator and external iliac nodes are commonly involved in 50% and 60% of cases, respectively [22] (Fig. 3). In 10%–30%, the presacral or lateral sacral nodes are the sole sites of nodal disease.

Bladder cancer spreads to the paravesicle nodes, which drain into the obturator and external iliac nodes. The obturator nodes are involved in 75% of cases with nodal disease [22]. Disease can also spread into the hypograstric and presacral nodes. These pathways eventually drain into the common iliac and paraotic chain of lymph nodes.

Nodal dissemination arising from gynecological malignancies (cervical, ovarian, and uterine) follows a similar pattern, most frequently to the obturator nodes,

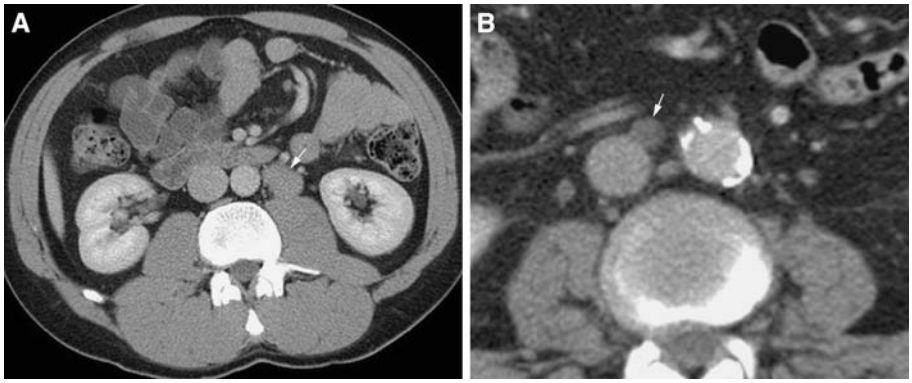

Fig. 4. Nodal spread from testicular tumor demonstrated on CT. (**A**) Left-sided testicular tumor typically spreads to left para-aortic node (*arrow*). (**B**) Right-sided tumors usually spread to precaval, retrocaval, paracaval, or aortocaval (*arrow*) nodes.

which is part of the medial chain of the external iliac nodes. From here, further spread occurs along the common iliac vessels into the retroperitoneum. Nodal spread can also involve the hypogastric nodes along the internal iliac vessels. Less commonly, tumor can track along the uterosacral ligament into the lymphatic plexus anterior to the sacrum and coccyx, which in turn drain into the common iliac nodes located between the common iliac arteries [23].

In colorectal cancer, right-sided tumors disseminate along lymph nodes following ileocolic vessels to the level of the superior mesenteric vein. Left-sided colonic tumors spread to lymph nodes along the inferior mesenteric vessels. Rectal cancers most commonly disseminate to mesorectal nodes and then upward to nodes along the superior rectal vessels. Of interest is that compared with diverticulitis, colonic cancer is more likely to result in enlargement of pericolic mesenteric lymph nodes [24].

In patients with testicular cancer, lymphatic spread of disease occurs along lymphatics channels that accompany the spermatic cord. These lymphatic vessels drain into nodes within the retroperitoneum. Typically, right-sided testicular tumors would disseminate to the retroperitoneal nodes on the right (the precaval, paracaval, aortocaval, and retrocaval nodes). Left-sided testicular tumors spread to nodes on the left (preaortic and paraortic nodes), usually at or just below the level of the left renal vein (Fig. 4). Crossover of nodal involvement can sometimes be seen, more frequently from the right to the left. More unusually, disease may spread to the so-called "echelon nodes," which lie anterior to the iliopsoas muscle (Fig. 5).

The nodal pathway for malignancy (gastric, pancreatic, liver, gallbladder, and bile ducts) in the upper abdomen is usually into the hepatoduodenal, peripancreatic (Fig. 6), and aortocaval nodes [25]. These may be involved singly or in combination, representing the flow of lymphatics from the lesser omentum into the retroperitoneal. The lymphatic drainage for the kidneys is variable but generally follows the ipsilateral renal vein to the paraortic/paracaval lymph nodes.

Fig. 5. CT imaging through the abdomen shows a left "echelon" node (*arrow*) lying anterior to the left psoas muscle in a patient with nonseminomatous germ cell tumor of the left testis.

The most common site of nodal dissemination in patients with vulval, penile, and anal cancer is to the inguinal nodes (Fig. 7).

Details of previous therapy (surgery, chemotherapy, or radiotherapy)

Knowledge of previous treatment is important since therapy can modify the pattern of nodal disease encountered. In prostate cancer, nodal relapse usually occurs outside the pelvis following radiotherapy or radical prostatectomy [15]. Similarly, following radical cystectomy for bladder cancer, nodal relapse is more frequently encountered within the hypogastric (internal iliac), presacral, and paraortic nodes [26] (Fig. 8). These represent nodal sites that are not usually subject to nodal dissection at surgery.

In patients with germ cell tumor of the testes, pelvic nodes are not usually involved except when (a) there has

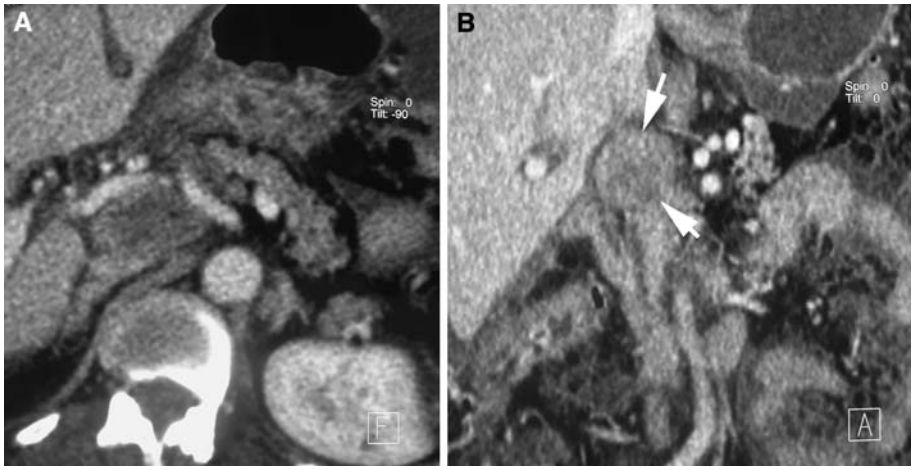

Fig. 6. (**A**) A peripancreatic lymph node may be difficult to distinguish from a mass lesion arising within the pancreas on axial CT imaging. (**B**) However, the use of multiplanar reformats in the coronal planes allows the anatomical location of the nodal mass (*arrows*) to be clearly defined.

been previous scrotal surgery, (b) the tumor arose in an undescended testis, (c) the involvement results from retrograde lymphatic spread due to bulky retroperitoneal nodal disease, or (d) there has been previous retroperitoneal nodal dissection (Fig. 9) [27].

Following total mesorectal excision surgery for rectal cancer, nodal recurrence can occur within the obturator chain or higher within the retroperitoneum.

CT and MRI findings

Unfortunately, the CT and MRI findings for malignant lymph nodes are frequently nonspecific. The most widely used criterion to determine whether a node is benign or malignant is nodal size. However, a substantial proportion of nodes harboring metastases from pelvic and abdominal cancers is not enlarged beyond the accepted size for normality. Furthermore, nodal enlargement can result from reactive nodal hyperplasia or coincidental diseases. Hence, when using cross-sectional imaging to evaluate nodal disease, the following parameters should be assessed in parallel to optimize our ability to detect malignant nodes.

Site

Nodes should be evaluated to determine if they conform to the anatomical position of pathway of spread for the primary tumors. Hence, the importance of a sound knowledge of the pathway of nodal dissemination cannot be overemphasized.

Size

The upper limit of maximum short-axis diameter deemed normal for nodes in the abdomen and pelvis is summarized in Table 1. Nodes measuring > 8 mm in maximum short-axis diameter on CT and MRI in the pelvis should be considered enlarged. In the abdomen, for the majority of cancers, a threshold > 10 mm in maximum short-axis diameter is considered pathological.

Fig. 7. Vulval, penile, and anal cancers most frequently disseminate to inguinal nodes. CT demonstrates a malignant, 3.5-cm, heterogeneously enhancing left inguinal node (*arrow*) with central low density. Note the associated stranding and infiltration in the subcutaneous tissue.

Nevertheless, the size criteria applied can vary between cancers. A study evaluating different size criteria (4, 6, 8, and 10 mm) for the detection of nodal metastasis in testicular cancer [28] showed that using a size threshold of 10 mm resulted in a sensitivity of 37% and a specificity of 100%. However, with a 4-mm criterion, the sensitivity was 93% and the specificity was 58%. Hence, using a smaller size criterion resulted in a reduction in the false-negative rate of nodal detection, although this was accompanied by diminished specificity [28]. In our practice, in the evaluation of a patient with testicular cancer, a node measuring > 10 mm in maximum short-axis diameter is considered to be definitely malignant,

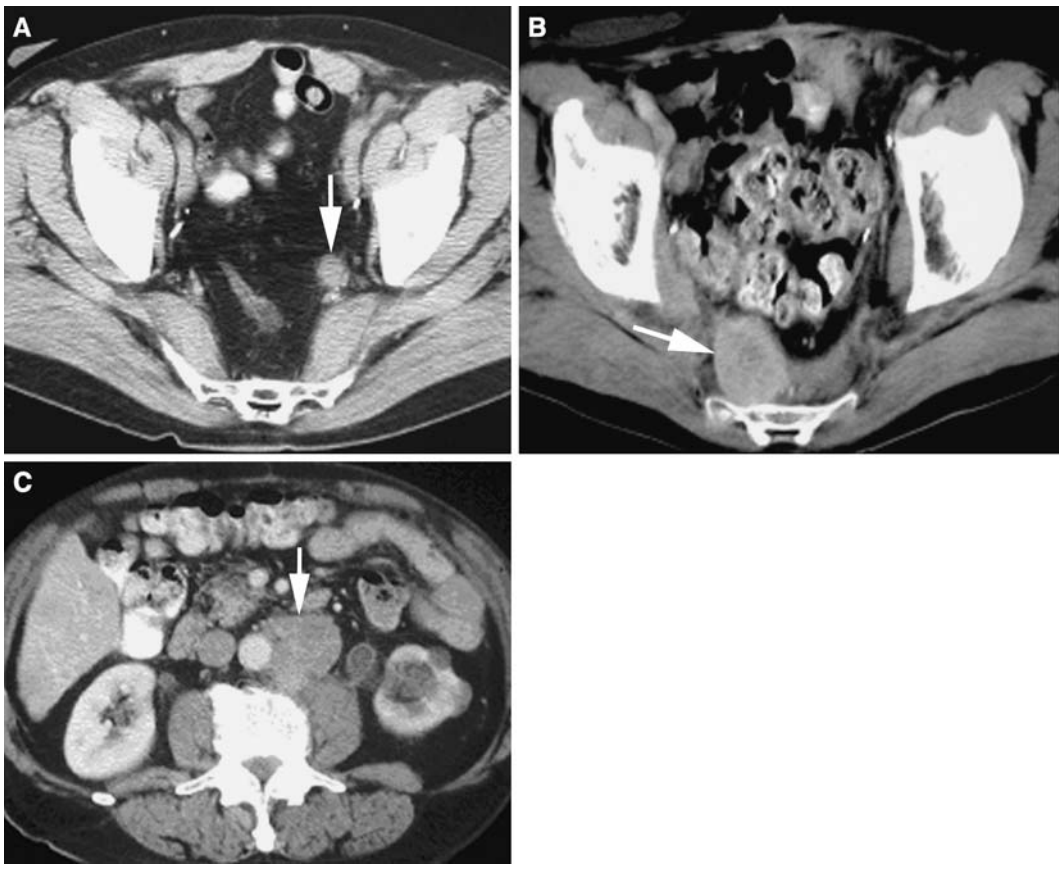

Fig. 8. CT imaging of nodal relapse in bladder cancer following radical cystectomy. Nodal relapse (*arrows*) may be observed within the (**A**) internal iliac node, (**B**) presacral node, and (**C**) retroperitoneal node. The retroperitoneal node may be the sole site of nodal relapse in 10% of these patients. Note also the heterogeneous enhancement associated with the larger nodes in b and c.

whereas a node that is between 8 and 10 mm in diameter is considered suspicious (Fig. 10).

Studies in prostate cancer have also shown that by reducing the threshold of size used, it was possible to improve the sensitivity but at a risk of reducing the specificity. Oyen et al. showed that by using 6 mm as the upper limit of normal on CT, it was possible to achieve a sensitivity of 78% and specificity of 97% in patients with prostate cancer [29]. In the same study, it was found that the specificity could be improved further by performing cytology from suspicious nodes > 6 mm in diameter [29].

Shape and contour

With the application of multidetector CT, which offers near-isotropic multiplanar reconstruction, the shape and contour of nodes can now be readily studied and can aid in assessment. Round (spherical) nodes have been found more likely to be malignant compared with ovoid nodes. This radiological sign has been validated on sonographic examination, where nodes showing a long-axis versus short-axis diameter of < 2 mm are more likely to be malignant [30]. However, the usefulness of this sign on CT is less certain.

In gastric cancer, it has been shown that malignant nodes have a significantly higher short- to long-axis ratio (0.81 versus 0.57), suggesting the usefulness of this sign

Fig. 9. In this 30-year-old with previous retroperitoneal dissection for right testicular nonseminomatous germ cell tumor, nodal relapse occurred within a right external iliac node (*arrow*). Pelvic nodal disease is unusual in patients with testicular cancer at presentation.

[31]. However, Lien et al. [32] found that a rounded node of < 20 mm on CT was not a good predictor of malignancy in patients with early-stage nonseminomatous testicular tumor. Nodal shape was also shown to be

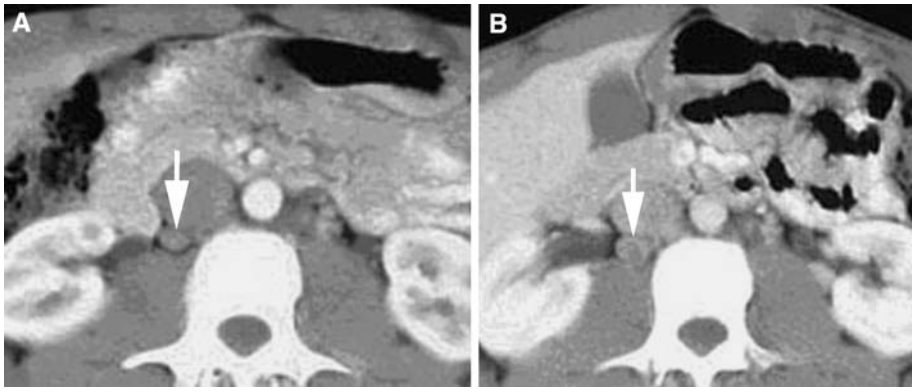

Fig. 10. The threshold of size at which a node is considered suspicious may be dependent on the disease and clinical context. In this man on surveillance for treated stage I right testicular cancer, (**A**) CT imaging revealed an 8-mm retrocaval lymph node (*arrow*), which was deemed equivocal. (**B**) Repeat CT imaging at 9 months revealed interval enlargement of the node (*arrow*) to 10 mm in maximum short-axis diameter, indicating nodal relapse.

Fig. 11. Nodal outline. In this man with rectal cancer, high-Gų spatial resolution, T2-weighted MRI demonstrates a 4-mm node (*circled*) posterior to the rectum, with irregular outlines indicating extracapsular extension of metastasis. By comparison, a benign 4-mm node with a smooth contour (*arrow*) is also visible within the perirectal fat.

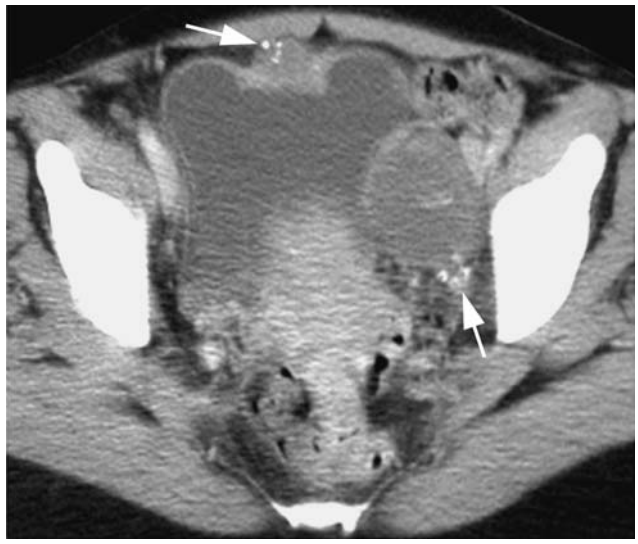

Fig. 12. Nodal calcification. In this man with a small transitional carcinoma arising from the anterior wall bladder wall, note the large left external iliac lymph node. The appearance of the node parallels that of the primary tumor in CT density. Calcification (*arrows*) is also visible in both the primary tumor and the metastatic lymph node.

unhelpful in the evaluation of nodal disease in pancreatic cancer [33].

Malignant nodes can exhibit irregular borders related to extracapsular extension of disease (Fig. 11). On MRI, irregular nodal contour has been found to be more accurate than nodal size in determining involvement of mesorectal nodes in patients with rectal cancer [3].

Number of nodes

A cluster of otherwise normal-appearing nodes may suggest malignancy. For example, in patients with non-Hodgkin lymphoma, a cluster of pathological nodes can sometimes be seen within the root of the small bowel mesentery. However, the specificity of the sign is low and can cause a false-positive result [34], particularly in the pelvis, where nodal asymmetry in not uncommon.

Internal nodal architecture

There are a number of internal nodal architectural features on CT and MRI which may be helpful in determining metastatic involvement.

a. *Calcifications*. Calcifications may be observed within metastatic nodes arising from ovarian, colorectal, breast, and bladder cancers (Fig. 12). Nodes may also show calcifications following treatment. This is frequently observed in lymphoma and seminoma.
b. *Heterogeneous appearance*. Large metastatic nodes frequently appear heterogeneous in density on CT (Fig. 7). The relatively lower-density center may result from necrosis. On MRI, the detection of central necrosis, which typically returns a high T2 signal, was found to have a very high positive predictive value in

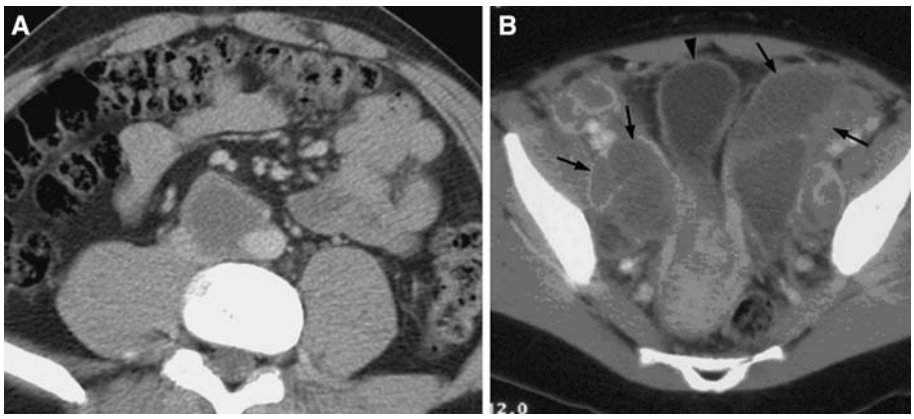

Fig. 13. Cystic-appearing lymph nodes. (**A**) Nodal metastasis arising from a nonseminomatous germ cell tumor of the testes frequently shows central low-density on CT imaging. However, this appearance is nonspecific and can be seen in certain infective conditions. (**B**) In another patient with tuberculous lymphadenitis, note the numerous enlarged cystic external iliac nodes (*arrows*), which appear similar in CT density to the urinary bladder (*arrowhead*).

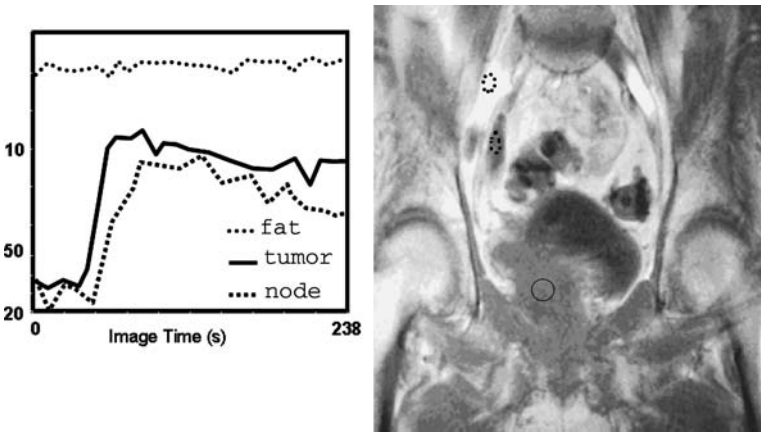

Fig. 14. Dynamic nodal enhancement. Graphs showing the uptake of gadolinium-DTPA contrast, with regions of interest drawn over fat, tumor, and lymph node. Note that the nodal contrast uptake parallels that of the primary tumor.

patients with cervical cancer [35]. In patients with rectal cancer, nodal heterogeneity is a feature of malignant mesorectal lymph nodes on high–spatial resolution T2-weighted MRI [3].

c. *Low-density "cystic" appearance*. Metastatic nodes arising from nonseminomatous germ cell tumor of the testes frequently exhibit a central low-density appearance on CT imaging [36] (Fig. 13). These nodes typically exhibit a high signal intensity on T2-weighted MRI. There is also evidence to show that solid to cystic change within a node following chemotherapy in a patient with nonseminomatous germ cell tumor is likely to represent mature differentiated teratoma [37]. Nevertheless, low-density nodes are not pathognomonic of malignant infiltration, as they may also be observed in infectious conditions such as tuberculosis and fungal infections (Fig. 13).

d. *Contrast enhancement*. Lymph nodes are frequently enhanced with contrast. Inhomogeneous enhancement of an enlarged node is more likely to indicate malignant infiltration [38, 39] (Fig. 14). Uniform homogeneous nodal enhancement may, however, result from both benign and malignant conditions [38, 39]. Metastatic nodes can show contrast enhancement that parallels the enhancement of the primary tumor and may reflect the grade and aggressiveness of the primary tumor [40].

More recently, it has been shown that it is possible to discriminate between benign and malignant nodes based on semiquantitative or quantitative analysis of the rate of nodal contrast enhancement on both CT and MRI [38] (Fig. 18). Nevertheless, this approach is still largely confined to the research arena and is not yet widely practiced due to the considerable demands on time and expertise.

e. *Nodal signal characteristics on MRI*. Apart from specific instances described above, the signal characteristics of lymph nodes are not useful for discriminating between malignant and benign nodes on MRI. It has also been found that it is not possible to distinguish between malignant and benign lymph nodes by measuring the T1 and T2 relaxation times of the nodes [41].

f. *Fat density*. The presence of fat density within a node indicates benignity (Fig. 15).

Diagnostic accuracy of cross-sectional imaging for nodal staging

Overall, the diagnostic accuracy of CT and MRI for nodal staging of cancers in the abdomen and pelvis varies widely in the reported literature. For pelvic malignancies, the accuracy of CT and MRI is similar [42–44]. The reported sensitivities range from 40% to 87%, and the

Fig. 15. Fat density in lymph nodes. CT imaging in this lady with breast cancer shows a 1.8-cm node in the left para-aortic space (*arrow*). Note the presence of a fatty nodal hilum, suggesting benignity. The CT appearance was unchanged on follow-up imaging.

specificities from 64% to 100% [29, 42–48]. The diagnostic performance of CT and MRI in the upper abdomen for nodal staging is also limited. In one study of gastric cancer, the accuracy of nodal staging using CT and MRI was 58% and 55%, respectively [17]. In another study of pancreatic cancer, a sensitivity of 14%, specificity of 85%, and accuracy of 73% were achieved for nodal staging [33].

Both conventional CT and MRI are limited by their ability to detect metastases in normal or minimally enlarged lymph nodes. The ability to detect nodes has to be tempered against the clinical importance of detection. For example, in patients undergoing radical prostatectomy and nodal dissection for prostate cancer, the diagnosis of metastatic nodal involvement may preclude surgery and a high specificity is therefore required. By comparison, nodal staging may be less important in another patient who would be treated by radical radiotherapy for advanced local disease.

Pitfalls in diagnosis

Normal structures and other pathological processes can mimic nodal disease. While many of these pitfalls can now be overcome by the use of thin-section multichannel CT with multiplanar reformats, some of these can still occasionally cause errors in interpretation. Hence, awareness of the range and variety of the anatomical structures or disease entities that can simulate nodal disease is important. The common pitfalls in the diagnosis of nodal disease in the abdomen and pelvis are as listed below.

a. *Loops of bowel*. Small bowel loops in close proximity to the retroperitoneum can simulate nodal disease.
b. *Normal ovaries*. Normal ovaries can simulate external iliac nodal enlargement. However, these lie medial to the pelvic fascia and the position of the ureter. By comparison, the external iliac nodal chain is located lateral to the parietal pelvic fascia and ureters.
c. *Vessels and aneurysms*. Blood vessels are most frequently mistaken for lymph nodes. Within the pelvis, imaging should not be performed in the arterial phase since unopacified veins can simulate nodal disease [49]. In the abdomen, unopacified small lumbar veins likewise can simulate nodal disease. Normal anatomical variants such as left-sided inferior vena cava or duplicated vena cava can mimic nodal enlargement. Aneurysmal dilatation of iliac vessels can also be confused with nodal enlargement, especially on non–contrast enhanced imaging. In addition, a prominent cisterna chyli can simulated retrocrural nodal enlargement [50] (Fig. 16).
d. *Lymphocoele*. Following surgery, lymphocoeles may simulate low-density nodal disease. However, knowledge of the site of surgical dissection can help a confident diagnosis to be made.
e. *Hematoma and abscess*. Postoperative hematomas or infective collection can also simulate nodal disease. Again, these resolve with time and can be confirmed on follow-up imaging.
f. *Nerves*. The nerves arising from the hypogastric plexus may simulate nodal disease. In addition, neurogenic tumors, such as neurofibromas, may also be confused with enlarged nodes (Fig. 17).

New approaches to nodal imaging

Dynamic CT or MRI may be used to evaluate the uptake of contrast medium into lymph nodes, providing information relating to the vascularity of these nodes [41]. It has been shown that tumor tissue is characterized by rapid contrast uptake followed by contrast washout. The kinetics of the contrast passage through a lymph node can be visualized by drawing a region of interest around a node and plotting the change in the CT enhancement value or the MR signal intensity with time. These data can be also be subjected to more complex mathematical modeling, which allows quantitative parameters that reflect vascular permeability and vascular blood volume to be derived.

The enhancement characteristics of malignant nodes differ from those of normal nodes and can allow these to be distinguished. Changes in the vascular properties of nodes may potentially be detected following treatment with chemotherapy or antiangiogenic agents, prior to a change in nodal size, thus providing a surrogate marker for early treatment response.

More recently, lymphotrophic MR contrast agents have been applied to the evaluation of abdominal and pelvic lymph nodes on MRI [51–55]. The most widely

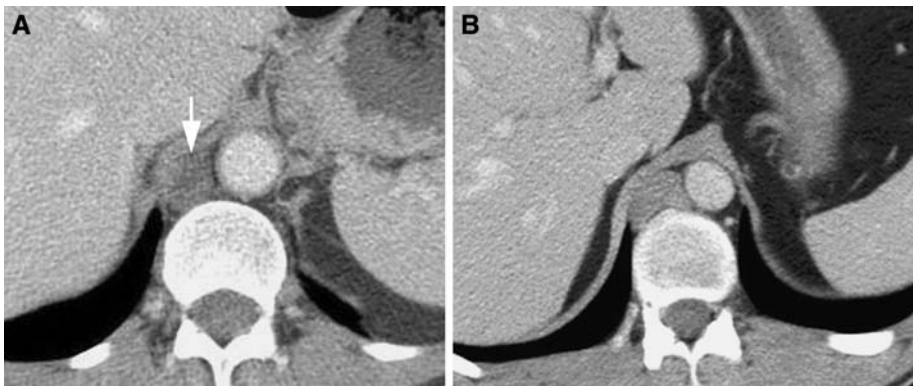

Fig. 16. (**A**) A prominent cisterna chyli (*arrow*) can simulate (**B**) a retrocrural node (*arrow*) on CT imaging. However, note that the cisterna chyli approximates fluid density on imaging, whereas a node is usually of higher soft tissue attenuation.

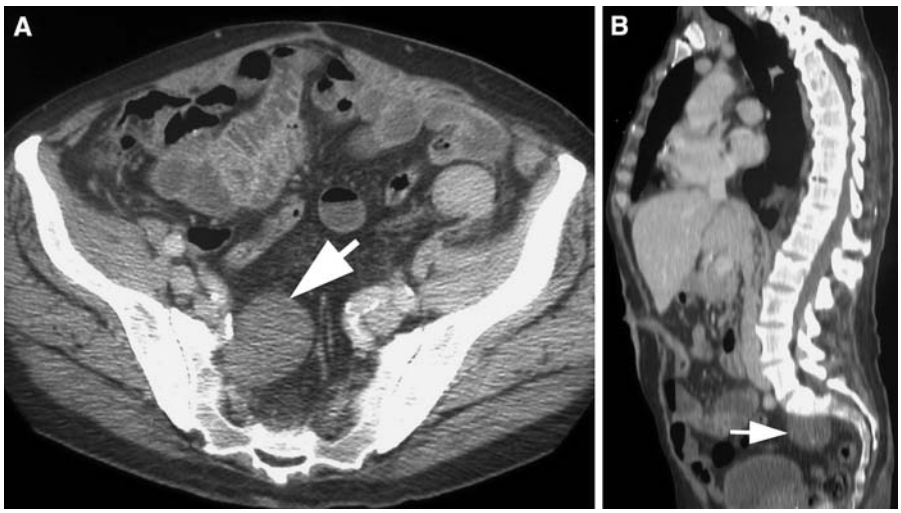

Fig. 17. A peripheral nerve sheath tumor (*arrow*) can simulate pelvic sidewall nodal disease in CT. However, in this example, the use of sagittal reformat shows the relationship of the mass (*arrow*) to the sacrum.

evaluated lymphotrophic contrast is ultrasmall iron oxide particles (USPIO). The contrast is taken up by normal nodal macrophages, which results in signal loss in normal nodes on T2*-weighted MRI (Fig. 18). Malignant nodes, being macrophage depleted, maintain a high signal intensity on the postcontrast scan. Early experience in the use of the agent has demonstrated a high sensitivity and specificity for nodal staging in prostate cancer [53].

With the increasing availability of positron emission tomography (PET), the role of PET/CT in the evaluation of nodal disease is evolving (Fig. 19). PET imaging has been shown to be useful in diagnosing nodal disease [56, 57]. However, more importantly, PET/CT has been shown to be useful in monitoring the effects of treatment in patients with lymphoma and testicular cancers [58–60].

Conclusions

Cross-sectional CT and MRI are helpful for the visualization of nodes within the abdomen and pelvis. Although the widely used size criterion is limited in its diagnostic accuracy, nodal staging using these techniques can be improved by having a clear knowledge and understanding of the underlying disease entities and by applying ancillary criteria in the interpretation of the images. However, novel imaging methods such as dynamic contrast enhanced imaging, MR lymphotrophic contrast agent imaging, and PET/CT are likely to have a significant impact on nodal imaging in the future.

References

1. Tiguert R, Gheiler EL, Tefilli MV, et al. (1999) Lymph node size does not correlate with the presence of prostate cancer metastasis. Urology 53:367–371
2. Lucey BC, Stuhlfaut JW, Soto JA (2005) Mesenteric lymph nodes: detection and significance on MDCT. AJR 184:41–44
3. Brown G, Richards CJ, Bourne MW, et al. (2003) Morphologic predictors of lymph node status in rectal cancer with use of high-spatial-resolution MR imaging with histopathologic comparison. Radiology 227:371–377
4. Jager GJ, Barentsz JO, Oosterhof GO, Witjes JA, Ruijs SJ (1996) Pelvic adenopathy in prostatic and urinary bladder carcinoma: MR imaging with a three-dimensional TI-weighted magnetization-prepared-rapid gradient-echo sequence. AJR 167:1503–1507
5. Dorfman RE, Alpern MB, Gross BH, Sandler MA (1991) Upper abdominal lymph nodes: criteria for normal size determined with CT. Radiology 180:319–322
6. Magnusson A (1983) Size of normal retroperitoneal lymph nodes. Acta Radiol Diagn (Stockh) 24:315–318
7. Einstein DM, Singer AA, Chilcote WA, Desai RK (1991) Abdominal lymphadenopathy: spectrum of CT findings. Radiographics 11:457–472

8. Vinnicombe SJ, Norman AR, Nicolson V, Husband JE (1995) Normal pelvic lymph nodes: evaluation with CT after bipedal lymphangiography. Radiology 194:349–355
9. Peters PE, Beyer K (1985) [Normal lymph node cross sections in different anatomic regions and their significance for computed tomographic diagnosis]. Radiologe 25:193–198
10. Balfe DM, Mauro MA, Koehler RE, et al. (1984) Gastrohepatic ligament: normal and pathologic CT anatomy. Radiology 150:485–490
11. Grey AC, Carrington BM, Hulse PA, Swindell R, Yates W (2000) Magnetic resonance appearance of normal inguinal nodes. Clin Radiol 55:124–130
12. Zirinsky K, Auh YH, Rubenstein WA, Kneeland JB, Whalen JP, Kazam E (1985) The portacaval space: CT with MR correlation. Radiology 156:453–460
13. Bundrick WS, Culkin DJ, Mata JA, Zitman RI, Venable DD (1993) Evaluation of the current incidence of nodal metastasis from prostate cancer. J Surg Oncol 52:269–271
14. Neal AJ, Dearnaley DP (1993) Prostate cancer: pelvic nodes revisited–sites, incidence and prospects for treatment with radiotherapy. Clin Oncol (R Coll Radiol) 5:309–312
15. Spencer J, Golding S (1992) CT evaluation of lymph node status at presentation of prostatic carcinoma. Br J Radiol 65:199–201
16. Sakuragi N, Satoh C, Takeda N, et al. (1999) Incidence and distribution pattern of pelvic and paraaortic lymph node metastasis in patients with Stages IB, IIA, and IIB cervical carcinoma treated with radical hysterectomy. Cancer 85:1547–1554
17. Sohn KM, Lee JM, Lee SY, Ahn BY, Park SM, Kim KM (2000) Comparing MR imaging and CT in the staging of gastric carcinoma. AJR 174:1551–1557
18. Brown G, Radcliffe AG, Newcombe RG, Dallimore NS, Bourne MW, Williams GT (2003) Preoperative assessment of prognostic factors in rectal cancer using high-resolution magnetic resonance imaging. Br J Surg 90:355–364
19. Nicolai N, Miceli R, Artusi R, Piva L, Pizzocaro G, Salvioni R (2004) A simple model for predicting nodal metastasis in patients with clinical stage I nonseminomatous germ cell testicular tumors undergoing retroperitoneal lymph node dissection only. J Urol 171:172–176
20. Marks LB, Rutgers JL, Shipley WU, et al. (1990) Testicular seminoma: clinical and pathological features that may predict paraaortic lymph node metastases. J Urol 143:524–527
21. Partin AW, Mangold LA, Lamm DM, Walsh PC, Epstein JI, Pearson JD (2001) Contemporary update of prostate cancer staging nomograms (Partin tables) for the new millennium. Urology 58:843–848
22. Golimbu M, Morales P, Al-Askari S, Brown J (1979) Extended pelvic lymphadenectomy for prostatic cancer. J Urol 121:617–620
23. Park JM, Charnsangavej C, Yoshimitsu K, Herron DH, Robinson TJ, Wallace S (1994) Pathways of nodal metastasis from pelvic tumors: CT demonstration. Radiographics 14:1309–1321
24. Chintapalli KN, Esola CC, Chopra S, Ghiatas AA, Dodd GD 3rd (1997) Pericolic mesenteric lymph nodes: an aid in distinguishing diverticulitis from cancer of the colon. AJR 169:1253–1255
25. Efremidis SC, Vougiouklis N, Zafiriadou E, et al. (1999) Pathways of lymph node involvement in upper abdominal malignancies: evaluation with high-resolution CT. Eur Radiol 9:868–874
26. Koh DM, Husband JE (2003) Pattern of disease recurrence of bladder carcinoma following radical cystectomy. Cancer Imaging 3:96–100
27. Husband JE, MacVicar D (1998) Testicular germ cell tumour. In: Husband JE, Reznek RH (eds) *Imaging in oncology*. ISIS Medical Media: Oxford, pp 259–276
28. Hilton S, Herr HW, Teitcher JB, Begg CB, Castellino RA (1997) CT detection of retroperitoneal lymph node metastases in patients with clinical stage I testicular nonseminomatous germ cell cancer: assessment of size and distribution criteria. AJR 169:521–525
29. Oyen RH, Van Poppel HP, Ameye FE, Van de Voorde WA, Baert AL, Baert LV (1994) Lymph node staging of localized prostatic carcinoma with CT and CT-guided fine-needle aspiration biopsy: prospective study of 285 patients. Radiology 190:315–322
30. Steinkamp HJ, Cornehl M, Hosten N, Pegios W, Vogl T, Felix R (1995) Cervical lymphadenopathy: ratio of long- to short-axis diameter as a predictor of malignancy. Br J Radiol 68:266–270
31. Fukuya T, Honda H, Hayashi T, et al. (1995) Lymph-node metastases: efficacy for detection with helical CT in patients with gastric cancer. Radiology 197:705–711
32. Lien HH, Lindskold L, Stenwig AE, Ous S, Fossa SD (1987) Shape of retroperitoneal lymph nodes at computed tomography does not correlate to metastatic disease in early stage non-seminomatous testicular tumors. Acta Radiol 28:271–273
33. Roche CJ, Hughes ML, Garvey CJ, et al. (2003) CT and pathologic assessment of prospective nodal staging in patients with ductal adenocarcinoma of the head of the pancreas. AJR 180:475–480
34. Matsukuma K, Tsukamoto N, Matsuyama T, Ono M, Nakano H (1989) Preoperative CT study of lymph nodes in cervical cancer—its correlation with histological findings. Gynecol Oncol 33:168–171
35. Yang WT, Lam WW, Yu MY, Cheung TH, Metreweli C (2000) Comparison of dynamic helical CT and dynamic MR imaging in the evaluation of pelvic lymph nodes in cervical carcinoma. AJR 175:759–766
36. Scatarige JC, Fishman EK, Kuhajda FP, Taylor GA, Siegelman SS (1983) Low attenuation nodal metastases in testicular carcinoma. J Comput Assist Tomogr 7:682–687
37. Husband JE, Hawkes DJ, Peckham MJ (1982) CT estimations of mean attenuation values and volume in testicular tumors: a comparison with surgical and histologic findings. Radiology 144:553–558
38. Barentsz JO, Jager GJ, van Vierzen PB, et al. (1996) Staging urinary bladder cancer after transurethral biopsy: value of fast dynamic contrast-enhanced MR imaging. Radiology 201:185–193
39. Noworolski SM, Fischbein NJ, Kaplan MJ, et al. (2003) Challenges in dynamic contrast-enhanced MRI imaging of cervical lymph nodes to detect metastatic disease. J Magn Reson Imaging 17:455–462
40. Husband JE, Koh DM (2004) Bladder cancer. In: Husband JE, Reznek RH (eds) *Imaging in oncology*. 2nd ed. Taylor and Francis: London, pp 343–374
41. Dooms GC, Hricak H, Moseley ME, Bottles K, Fisher M, Higgins CB (1985) Characterization of lymphadenopathy by magnetic resonance relaxation times: preliminary results. Radiology 155: 691–697
42. Kim SH, Choi BI, Lee HP, et al. (1990) Uterine cervical carcinoma: comparison of CT and MR findings. Radiology 175:45–51
43. Kim SH, Kim SC, Choi BI, Han MC (1994) Uterine cervical carcinoma: evaluation of pelvic lymph node metastasis with MR imaging. Radiology 190:807–811
44. Williams AD, Cousins C, Soutter WP, et al. (2001) Detection of pelvic lymph node metastases in gynecologic malignancy: a comparison of CT, MR imaging, and positron emission tomography. AJR 177:343–348
45. Fukuda H, Nakagawa T, Shibuya H (1999) Metastases to pelvic lymph nodes from carcinoma in the pelvic cavity: diagnosis using thin-section CT. Clin Radiol 54:237–242
46. Salo JO, Kivisaari L, Rannikko S, Lehtonen T (1986) The value of CT in detecting pelvic lymph node metastases in cases of bladder and prostate carcinoma. Scand J Urol Nephrol 20:261–265
47. Subak LL, Hricak H, Powell CB, Azizi L, Stern JL (1995) Cervical carcinoma: computed tomography and magnetic resonance imaging for preoperative staging. Obstet Gynecol 86:43–50
48. Sugiyama T, Nishida T, Ushijima K, et al. (1995) Detection of lymph node metastasis in ovarian carcinoma and uterine corpus carcinoma by preoperative computerized tomography or magnetic resonance imaging. J Obstet Gynaecol 21:551–556
49. Teefey SA, Baron RL, Schulte SJ, Shuman WP (1990) Differentiating pelvic veins and enlarged lymph nodes: optimal CT techniques. Radiology 175:683–685
50. Gollub MJ, Castellino RA (1996) The cisterna chyli: a potential mimic of retrocrural lymphadenopathy on CT scans. Radiology 199:477–480
51. Koh DM, Brown G, Temple L, et al. (2004) Rectal cancer: mesorectal lymph nodes at MR imaging with USPIO versus histopathologic findings—initial observations. Radiology 231:91–99
52. Bellin MF, Lebleu L, Meric JB (2003) Evaluation of retroperitoneal and pelvic lymph node metastases with MRI and MR lymphangiography. Abdom Imaging 28:155–163

53. Harisinghani MG, Barentsz J, Hahn PF, et al. (2003) Noninvasive detection of clinically occult lymph-node metastases in prostate cancer. N Engl J Med 348:2491–2499
54. Deserno WM, Harisinghani MG, Taupitz M, et al. (2004) Urinary bladder cancer: preoperative nodal staging with ferumoxtran-10-enhanced MR imaging. Radiology 233:449–456
55. Harisinghani MG, Saini S, Slater GJ, Schnall MD, Rifkin MD (1997) MR imaging of pelvic lymph nodes in primary pelvic carcinoma with ultrasmall superparamagnetic iron oxide (Combidex): preliminary observations. J Magn Reson Imaging 7:161–163
56. Reinhardt MJ, Ehritt-Braun C, Vogelgesang D, et al. (2001) Metastatic lymph nodes in patients with cervical cancer: detection with MR imaging and FDG PET. Radiology 218: 776–782
57. Horowitz NS, Dehdashti F, Herzog TJ, et al. (2004) Prospective evaluation of FDG-PET for detecting pelvic and para-aortic lymph node metastasis in uterine corpus cancer. Gynecol Oncol 95:546–551
58. Hutchings M, Eigtved AI, Specht L (2004) FDG-PET in the clinical management of Hodgkin lymphoma. Crit Rev Oncol Hematol 52:19–32
59. Burton C, Ell P, Linch D (2004) The role of PET imaging in lymphoma. Br J Haematol 126:772–784
60. Huddart RA (2003) Use of FDG-PET in testicular tumours. Clin Oncol (R Coll Radiol) 15:123–127
61. Graham RA, Garnsey L, Jessup JM (1990) Local excision of rectal carcinoma. Am J Surg 160:306–312
62. Herr HW (1988) Bladder cancer: pelvic lymphadenectomy revisited. J Surg Oncol 37:242–245
63. Lerner SP, Skinner DG, Lieskovsky G, et al. (1993) The rationale for en bloc pelvic lymph node dissection for bladder cancer patients with nodal metastases: long-term results. J Urol 149:758–764, discussion 764–755